Effects of Zone Drawing on the Structure of Metallocene Polyethylene

DAVID M. BERNS,[1] ELIZABETH OYEBODE,[1] BENITA DAIR,[1]* PEGGY CEBE,[1] MALCOLM CAPEL[2] †

[1] Department of Physics and Astronomy, Tufts University, Medford, Massachusetts 02155

[2] Biology Department, Brookhaven National Laboratory, Upton, New York, 11973

Received 21 December 2000; accepted 13 March 2001

ABSTRACT: The influence of zone drawing on bulk properties and structure of metallocene polyethylene (*m*-PE) is reported. Two different *m*-PE materials were subjected to tensile stresses above the yield point by zone drawing in the temperature range from 50 to 100°C. Drawn materials were characterized by using small- and wide-angle X-ray scattering (SAXS, WAXS), molecular retraction, and small-angle light scattering (SALS). Structural changes were studied as a function of drawing temperature, engineering stress, and draw ratio. WAXS showed strong crystalline orientation in drawn samples, and only the orthorhombic crystal modification was observed. SAXS showed lamellar orientation in drawn samples. At low drawing temperatures of 50 or 60°C, draw ratio increased as a step function of stress. There is a stress barrier, which must be exceeded before high-draw ratios can be achieved at these temperatures. At drawing temperatures of 70°C or above, the barrier stress is low enough that draw ratio increases nearly linearly as a function of stress. Below the stress barrier, spherulitic structure is observed by small-angle light scattering (SALS). Elongation occurs via deformation of the interspherulitic amorphous phase. Molecular retraction was low for these samples, indicating mostly plastic deformation of the amorphous material. Above the stress barrier, SALS showed that spherulites are destroyed. Elongation occurs via deformation of the intraspherulitic amorphous phase. Molecular retraction for these samples was high, indicating elastic deformation of the amorphous material. J Appl Polym Sci 82: 3492–3504, 2001

Key words: zone drawing; metallocene polyethylene; draw ratio; molecular retraction; X-ray scattering

INTRODUCTION

The relationship between mechanical properties and crystal structure in polyethylene (PE) has been studied extensively since the 1950s. By using transmission electron microscopy, Keller first enunciated the principle of chain-folded lamellar crystals as the underlying feature of polymer molecular organization and studied the arrangement of lamellae into spherulites.[1] Subsequent work by Keller's group included the study of the deformation of PE and its relationship both to lamellae and to spherulitic superstructure.[2–5] The literature in this area is vast, and we refer the reader to an excellent review of mechanical properties in which much of the early work of Keller's group and others is described.[6] Pope and Keller[3] exam-

Correspondence to: P. Cebe.

* *Present address:* W. R. Grace, Cambridge, MA.

† *Present address:* Advanced Photon Source, Argonne National Laboratory, Argonne, IL.

Contract grant sponsor: National Aeronautics and Space Administration; contract grant number: NAG8-1460; contract grant sponsor: U.S. Army Research Office; contract grant number: DAAH04-96-1-0009.

Journal of Applied Polymer Science, Vol. 82, 3492–3504 (2001)

ined the mechanisms of PE deformation and found that the crystallographic *c*-axis becomes oriented along the direction of applied stress, resulting in deformation of the stacks of lamellae. Three mechanisms of lamellar deformation were suggested: lamellar slip, chain slip, and lamellar separation.[3]

Lin and Argon[6] suggest the progression of plastic deformation in PE. The lower modulus amorphous phase deforms first, followed by deformation of the lamellae by the dominant mechanism of slip of the crystals along the plane containing the molecular chains. The spherulitic superstructure can deform either homogeneously or heterogeneously.[5] Under the former mechanism, yield can occur either at the boundary between adjacent spherulites (which we will call interspherulitic deformation) or in the equatorial regions. In the equatorial regions, the lamellae have their surface normals along the stress direction. Yield can occur by separation of lamellae in this region (which we will call intraspherulitic, or interlamellar, deformation), leading to an increase in the long periodicity, and by crystal rotation about the crystallographic *b*-axis.[6] The *b*-axis in PE is along the spherulite radius,[2] and thus, in the equatorial regions, the *b*-axis is perpendicular to the applied stress. Hay and Keller[5] found that the chain axis in PE could more easily rotate about the *b*-axis than about the *a*-axis.

Most prior studies were performed on PE synthesized by the Ziegler–Natta process (z-PE), which was the only material available until the last decade. Polymers prepared with Ziegler–Natta catalysts possess a broad molecular weight distribution (typically M_w/M_n is in the range of $\sim$ 8). With the advent of the transition metal catalysts, greater control over the molecular chain length became possible. Polyethylene prepared with transition metal catalysts (metallocene, or *m*-PE) has a much narrower molecular weight distribution, and M_w/M_n can be in the range of $\sim$ 2–3. Metallocene-synthesized PE can be expected to react differently to thermomechanical processes than the conventional Ziegler–Natta catalyzed polymers.

To produce uniaxially oriented materials with enhanced mechanical properties, the technique of hot drawing is usually applied to polymer films. Kunugi et al.[7] prepared ultra-high modulus polyethylene (*z*-PE) films by zone drawing single crystal mats. Yeh et al.[8] used one- and two-stage hot drawing to orient ultra-high molecular weight *z*-PE gels. Hoff and Pelzbauer[9,10] applied zone drawing to high-density *z*-PE to achieve films with very high birefringence and high orientation. Recently, Russell et al.[11] demonstrated the appearance of the monoclinic crystal phase in *z*-PE treated to a battering process. PE films are known to form the monoclinic crystal modification when subjected to mechanical stress beyond the yield point.[11,12]

In this article, we present results of the effects of zone drawing on the bulk properties and microscopic structure of *m*-PE. Two types of *m*-PE specimens were subjected to tensile stresses above the yield point by zone drawing. The process variables controlled in the experiment were the (variable) applied load and drawing temperature, and (constant) zone-heater speed. To characterize the materials before and after drawing, we used wide- and small-angle X-ray scattering (WAXS, SAXS), differential scanning calorimetry (DSC), analysis of draw ratio, molecular retraction, and small-angle light scattering (SALS). Because the *z*-PE and *m*-PE materials are different in their fundamental chain structures (i.e., they have different molecular lengths, length distributions, defect amount, and type), it is not possible to make a direct comparison of the drawing characteristics such as achievable draw ratio, or required drawing stress, because these depend strongly on molecular chain architecture. On the other hand, the crystalline structure, lamellar organization, and spherulitic superstructure are common to both *z*-PE and *m*-PE. Where possible, we compare the structure of the materials studied in this work with prior structural investigations on *z*-PE.

EXPERIMENTAL

The materials studied were Exceed 350D60 and Exceed 357C80, commercial *m*-PE received from Exxon, Baytown, TX. For the D60, Exxon reports a melt-flow index of 1.0, with M_n = 43,390 and M_w = 112,600 (M_w/M_n = 2.60).[13] The C80 is reported to have a melt-flow index of 3.4 with M_n = 31,960 and M_w = 73,060 (M_w/M_n = 2.29).[13]

The materials were received in pellet form and then compression molded at 200°C between ferrotype plates (lined with ULTEM™ polyether imide to facilitate removal of pressed material) and quenched with cold water. Gold fiduciary marks were then deposited on the sheets by thermal evaporation through a copper mesh with a very fine and well-known spacing. The samples used for drawing were cut from the marked sheets into

strips 150–300 μm thick, 0.63 cm wide, and 3 cm long, with their length parallel to the rows of gold marks.

Our zone-drawing apparatus was described previously[14] and follows the slotted heater design of Garrett and Grubb.[15] A heating element at constant temperature (T_d) was passed over the sample, with one surface in contact with the sample, at a constant speed of approximately 2 mm/s. At the same time, a force was applied to the sample by means of a free weight attached to the sample over a pulley.

The experiments consisted of drawing both D60 and C80 in the rubbery regime at 50, 60, 70, 80, 90, or 100°C. The maximum stress that could be applied to the samples was limited by the apparatus, which could only support masses of up to 2200 g. Samples were distinguished by three parameters: drawing temperature (T_d), engineering stress (σ), and draw ratio (λ). Engineering stress is the ratio of the free weight to the initial cross-sectional area of the sample. Draw ratio is defined as λ = (final length)/(initial length).

Many analysis tools were employed, including differential scanning calorimetry (DSC), which was performed by using a TA Instruments 2920 DSC at a heating rate of 10°C/min. Temperature calibration was performed with indium. The mass of drawn samples was between 1 and 4 mg and the samples were supported on a layer of oil in the DSC pans, loosely encapsulated without crimping the lids. The mass of undrawn samples was between 7 and 12 mg, and these were encapsulated in the normal way with crimped lids. Degree of crystallinity was determined from the endotherm area by using 293 J/g for the heat of fusion of 100% crystalline PE.[16]

The SALS setup consisted of a laser beam that passed through crossed polarizers (H_V pattern[17]) with the sample between them having its drawing direction parallel to the first polarizer. The exiting beam passed through a converging lens and the diffraction pattern was viewed on a ground glass plate located one focal length from the lens.

WAXS was performed by using a Philips PW 1830 X-ray generator and a Statton camera. The wavelength of radiation was 1.54 Å and the sample-to-detector distance was 2.97 cm, calibrated by using Si powder standard rubbed on the sample surface. The scattering data were recorded in transmission on Kodak Def 5 film.

SAXS measurements were taken at the National Synchrotron Light Source at Brookhaven National Laboratory on beam line X12B. Wavelength of radiation was 1.6 Å and the sample-to-detector distance was 180 cm, calibrated by using cholesterol myristate. The anisotropic scattering patterns were collected on a custom-built histogramming gas-filled 2-D wire detector.[18]

The molecular shrinkage was performed in a Mettler hot-stage where portions of drawn samples were heated above their melting point on the surface of an oil droplet. Retraction % (R) is defined as[19]:

$$R = \frac{(\text{drawn length} - \text{retracted length})}{(\text{drawn length} - \text{initial length})} \times 100 \quad (1)$$

All lengths are measured at room temperature. The initial length is the length of the sample before drawing, drawn length is the length of the zone-drawn sample before heating, and retracted length is the length of the zone-drawn sample after it was heated above the melting point.

RESULTS

Thermal Analysis and Wide-Angle X-ray Scattering

Thermal analysis by DSC, shown in Figure 1(a) (Curve A, D60 and Curve B, C80), reveals that both materials after compression molding (but before zone-drawing) had a single broad endotherm with an endothermic peak maximum at about 114°C. The initial pressed undrawn D60 or C80 sheets, from which samples were cut and drawn, had similar melting scans within experimental error. The heats of fusion for the initial pressed undrawn samples of D60 and C80 were 96.7 ± 4.0 and 92.4 ± 0.6 J/g, giving mass fraction degrees of crystallinity of 0.33 ± 0.01 and 0.31 ± 0.002, respectively. The error limits result from measurements on different pressings of the two materials.

Figure 1(a), Curves C and D, show D60 after drawing at 90°C to λ = 5.2 and λ = 6.5, respectively. The endotherms are sharper and less symmetric than in the undrawn samples. Also, the drawn samples are subject to spurious effects due to contraction of the fibers inside the DSC pans. In spite of the effort to eliminate this contraction, by loose encapsulation and flotation on an oil droplet, Curves C and D still exhibit some irregularities in endothermic response. At this high drawing temperature of 90°C, the area under the

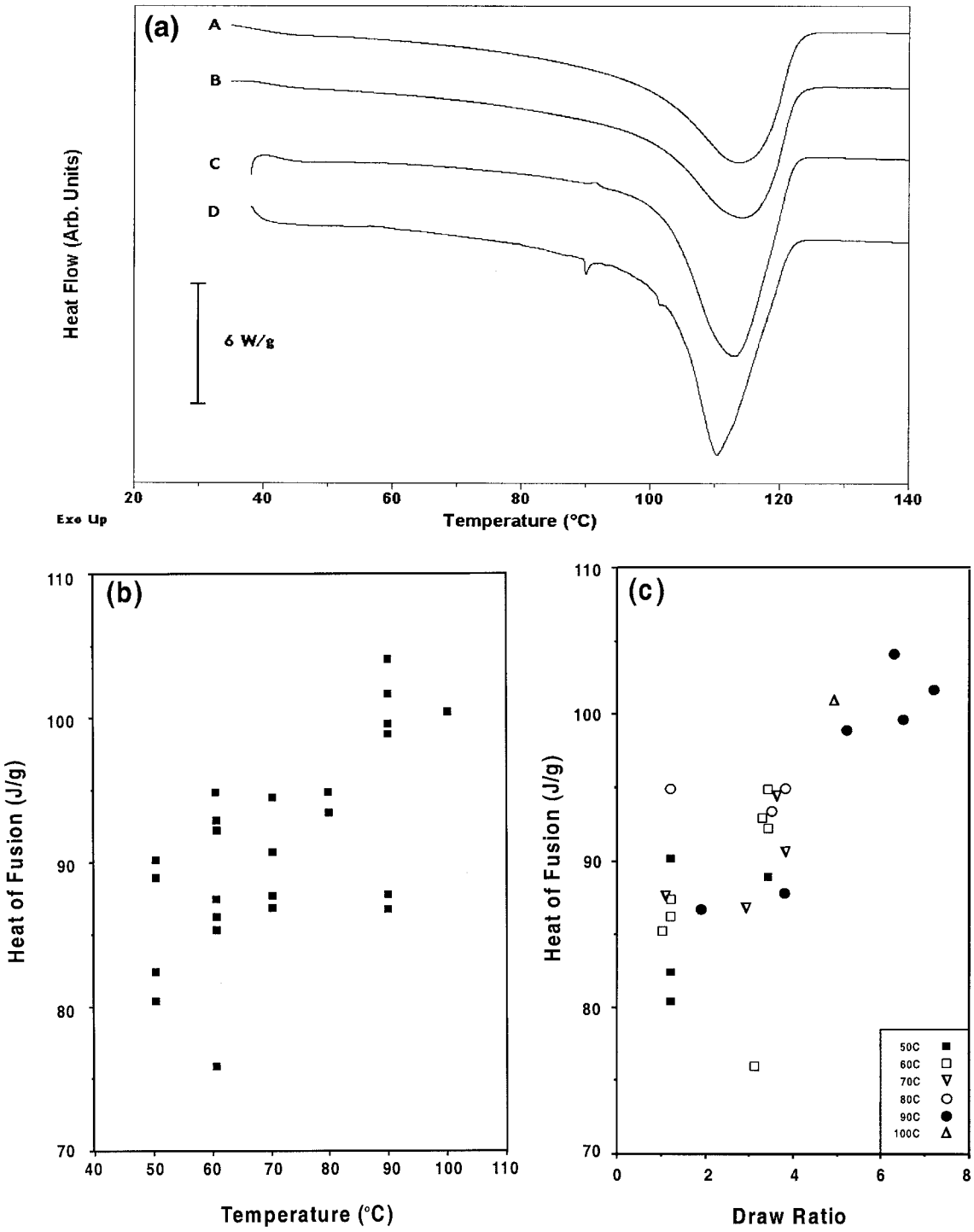

Figure 1 Thermal analysis results. (a) Endothermic heat flow versus temperature during DSC scanning at 10/min. Curve A, D60 before zone drawing; Curve B, C80 before zone drawing; Curve C, D60 drawn at 90°C to $\lambda = 5.2$; Curve D, D60 drawn at 90°C to $\lambda = 6.5$. Downward deflection represents endothermic response. (b) Heat of fusion versus drawing temperature for D60. (c) Heat of fusion versus draw ratio for D60 drawn at the temperatures indicated in the legend.

endotherm indicates a higher degree of crystallinity in these drawn samples than in the undrawn samples. However, this increase in crystallinity was not generally observed under other drawing conditions.

In fact, drawing at a lower temperature generally causes the degree of crystallinity to decrease. Figure 1(b) shows the variation in the heat of fusion as a function of drawing temperature for D60. The data are widely scattered but the following observations can be made. The heat of fusion generally increases as the drawing temperature increases. For 23 samples of D60 drawn in the temperature range from 50 to 90°C, 15 of these have measured heats of fusion less than the heat of fusion for the pressed but undrawn material. Only at the highest drawing temperatures of 90 or 100°C were heats of fusion found in excess of the average of the undrawn materials. Represented in this figure are samples having many different draw ratios and many different applied engineering stresses.

To separate the thermal effects (of heating during the zone drawing) from the application of stress, identical samples were heated inside the DSC with no stress applied. These samples were heated to the same zone-drawing temperature and held momentarily to mimic the heating during zone drawing, before being cooled rapidly. For the sake of brevity, we summarize the results of this test. A small low-temperature secondary endotherm was observed in these samples heated without drawing. The location of the secondary endotherm was about 15° above the highest treatment temperature. For D60 samples heated in the range from 50 to 100°C without drawing, the heats of fusion ranged from 100 to 107 J/g. For C80 samples heated in the range of 50–100°C without drawing, the heats of fusion ranged from 97 to 102 J/g. The lower overall crystallinity in C80, compared with D60, is consistent with the reduced crystallinity of the initial compression-molded, undrawn materials. For both materials, heating alone from 50 to 80°C causes the crystallinity to increase. Because the compression-molded samples were quickly cooled, brief exposure to elevated temperature causes an annealing of the crystals and slight increase in overall crystallinity. Application of both heat and drawing stress during zone drawing in this temperature range cause the crystallinity to decrease. Apparently, the drawing stresses result in a reduction of the crystal content at low T_d. Above 80°C, crystallinity increases as a result of either temperature or drawing stress.

Figure 1(c) shows the heat of fusion plotted as a function of draw ratio for D60. These samples experienced different drawing temperatures, as indicated, and different applied stresses and are the same samples shown in Figure 1(b). The general trend is for the heat of fusion to increase with increasing draw ratio. However, samples that were drawn to very low draw ratios, under $\lambda = 1.5$, showed a very wide spread in the heat of fusion. Only draw ratios of 4.0 or greater resulted in heats of fusion above 98 J/g. Effects of the drawing temperature may be summarized as follows. Of 12 samples with heats of fusion 91 J/g or smaller, 10 had been drawn at lower temperatures of 50, 60, or 70°C, while only five of thirteen samples with heats of fusion greater than 91 J/g had been drawn at these lower temperatures. The use of 91 J/g for this comparison was not arbitrary: it represents the largest heat of fusion of drawn samples that was still smaller than the heat of fusion of the initial undrawn, compression-molded films.

Analysis of the undrawn and drawn samples was performed using X-ray scattering. The undrawn samples were semicrystalline with no preferred crystalline orientation, as confirmed by WAXS. Only the orthorhombic crystal modification was observed.[20] These undrawn samples showed spherulitic superstructure when examined using SALS.

For the zone-drawn samples, WAXS showed a fiber-type, or uniaxial, diffraction pattern with strong crystalline orientation in the neck region of drawn samples where deformation is complete. Again, only the reflections characteristic of the orthorhombic phase were seen. No monoclinic crystal phase was identified in the zone-drawn samples, and no intensity was seen on the meridian. These results are similar to those of Sabbagh and Lesser on *m*-PE,[21] who found a random *c*-axis orientation in the undrawn material, and *c*-axis predominantly along the stress direction in the neck region of drawn samples.

Figure 2 shows a plot of the angular spread, α (in degrees), of D60 WAXS equatorial reflections plotted as a function of T_d, for a constant engineering stress. The three main equatorial reflections had Miller Indices of (110), (200), and (210).[11,12] At a constant engineering stress of 11.6 MPa, an increase of T_d results in an increase in draw ratio. Thus, the draw ratio increases from 3.4 at 50°C to 5.9 at 80°C. The increase in draw

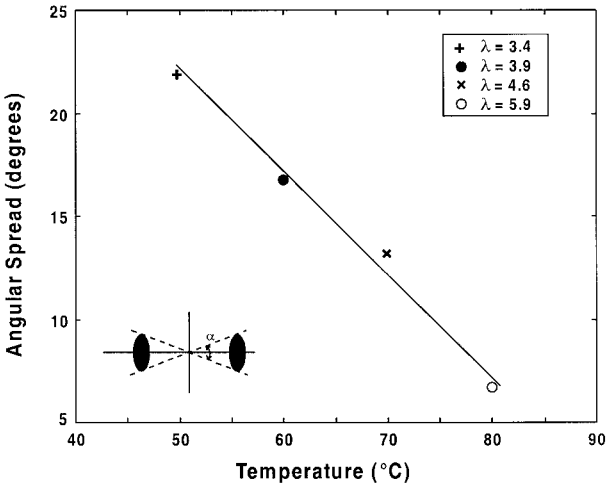

Figure 2 Angular spread, α, of the WAXS equatorial reflections versus drawing temperature for D60 at the draw ratios indicated. Drawing performed at a constant stress of 11.6 MPa.

ratio at constant stress results in a decrease in the angular spread of the reflections, indicative of higher orientational order of the crystallites. Though not pictured in Figure 2, WAXS revealed that the crystallites become oriented in D60 and C80 (albeit to a lesser extent) even at relatively low draw ratios, when $\lambda = 1.1$.

Analysis of Draw Ratio and Molecular Retraction

Figure 3 is a plot of engineering stress versus drawing temperature for D60 samples which were drawn to two draw ratios, $\lambda = 3.4$ and $\lambda = 4.5$. Engineering stress decreases linearly with drawing temperature, changing by about a factor of 2 from the lowest to highest temperature at a constant draw ratio. As drawing temperature increases, a reduced stress is needed to achieve the same draw ratio. An increase in engineering stress at a constant drawing temperature results in a higher draw ratio.

Figure 4(a–c) shows plots of draw ratio versus applied engineering stress for D60 (squares) and C80 (circles) drawn at $T_d = 60$, 90, and 100°C, respectively. The open symbols represent samples in which, by using SALS, spherulitic four-lobed patterns were observed, whereas the solid symbols represent samples in which no spherulites were observed. The role of the spherulites will be considered more fully later on in this section. From Figure 4(a), we see that drawing D60 at a low temperature of 60°C (and also at $T_d = 50$°C, which is not shown for brevity) results in draw ratios below 4.5 for all stresses used. Very low draw ratios, $\lambda = 1.0$–1.3, were observed for low engineering stresses in the range from 5 to 8 MPa. When the engineering stress increased to 9–10 MPa, variable draw ratios were observed. An increase in draw ratio of the D60 to $\lambda = 2.7$–4.0 was seen in some samples, whereas others did not draw significantly. For stresses greater than about 10 MPa, all samples had draw ratios above 2.7. With an increase of stress to 15 MPa, one sample drew to $\lambda \sim 4.4$, the largest draw ratio that could be obtained at this low drawing temperature. The C80 displayed a pattern of draw ratio versus applied stress similar to that seen in the D60. At lower stresses, only draw ratios in the range of $\lambda = 1.0$–1.3 were observed, whereas at higher stresses $\lambda = 3.5$–5.1 was achieved. However, a closer comparison of the two materials at $T_d = 60$°C reveals that at the higher stresses, the C80 nearly always had higher draw ratios than the D60 when comparing the same applied stress. For both D60 and C80, at low drawing temperatures of 50 and 60°C, neither material achieved significant draw ratio until the stress exceeded about 9–10 MPa, which is close to the reported yield stress of 8.4–8.8 MPa at room temperature.[22]

In Figure 4(b), we see that drawing D60 (squares) and C80 (circles) at a higher temperature of 90°C (and similarly at $T_d = 70$ and 80°C, which are not shown) results in a linear increase

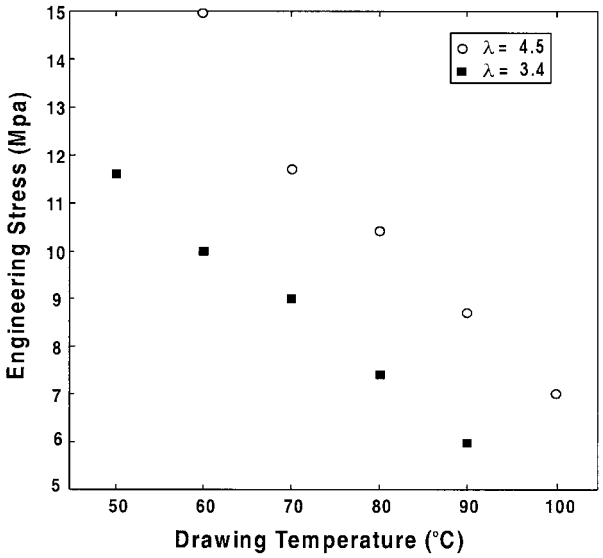

Figure 3 Drawing stress versus drawing temperature for D60 at two draw ratios: $\lambda = 3.4$ (solid squares); $\lambda = 4.5$ = (open circles).

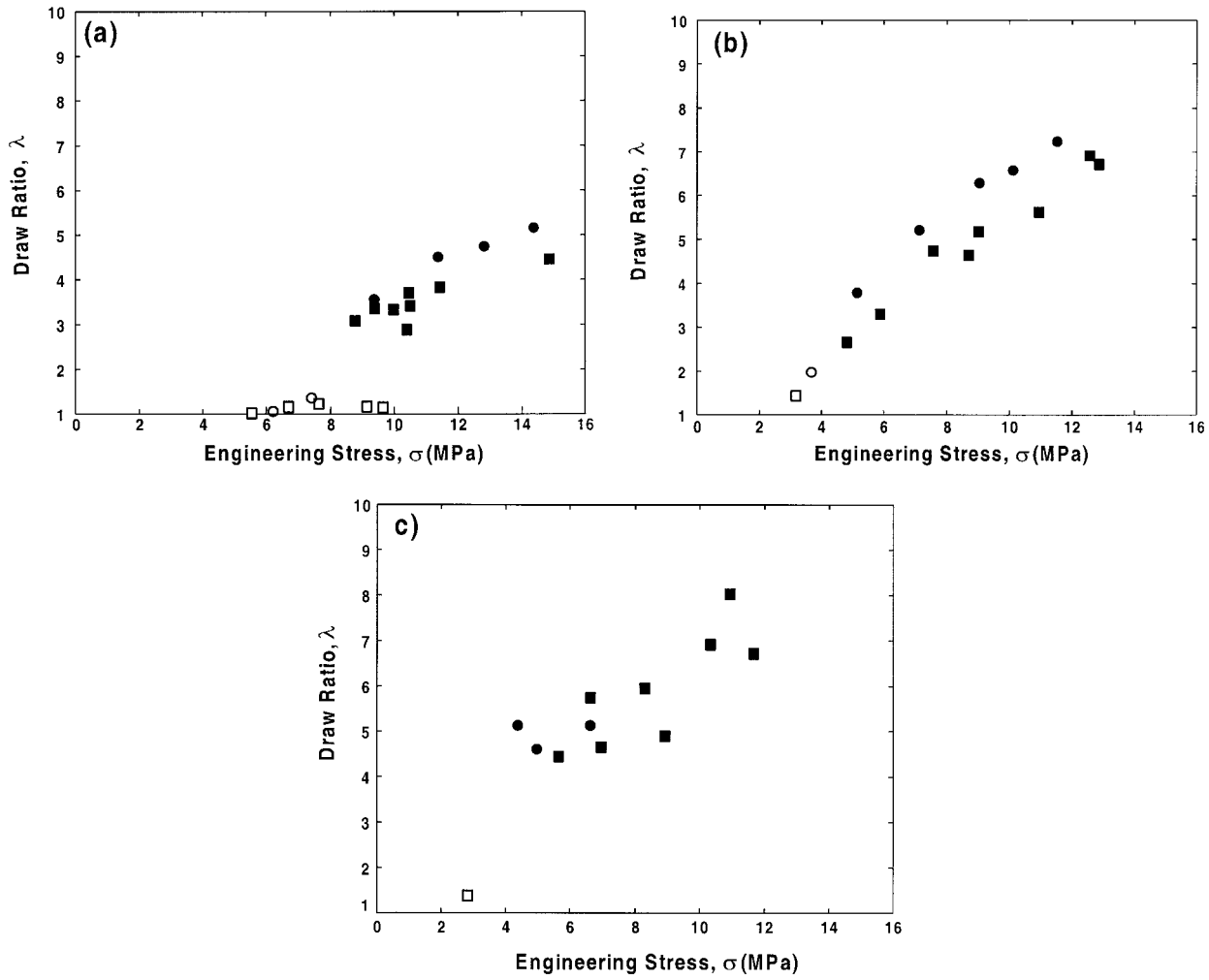

Figure 4 Draw ratio versus engineering stress for D60 (squares) and C80 (circles) at drawing temperatures of (a) 60°C; (b) 90°C; and (c) 100°C. Observation by light scattering revealed spherulites (open symbols) or no spherulites (solid symbols).

of draw ratio with engineering stress. For D60, draw ratio ranges from 1.4 to 6.5 for engineering stresses from 3 to 13 MPa. Once again, at higher stresses, the C80 achieves higher draw ratios than the D60 drawn at the same stress. The higher draw ratios for the C80 probably arise from the fact that it has a higher number density of chain ends and lower number of entanglements than the D60.

Very similar trends were seen in D60 and C80 drawn at 100°C, the highest temperature used in this work. These results are shown in Figure 4(c) and indicate that there is a greater variability of draw ratio with stress at this temperature. The drawing behavior of C80 at 100°C was different than the C80 drawn at the other high temperatures (70–90°C). At 100°C, the C80 was very hard to draw without breaking, and samples usually snapped during drawing. Inability to draw at the highest temperature can be understood from C80's higher melt-flow index and reduced molecular weight.

In summary, for both D60 and C80 at low drawing temperatures of 50 and 60°C, high draw ratios are only achieved after a stress barrier is overcome. At higher temperatures of 70, 80, 90°C (and for D60, 100°C), samples drew uniformly with a nearly linear increase in draw ratio with applied stress. At the highest drawing temperature of 100°C, C80 failed to draw most of the time.

In an attempt to understand why there seems to be a barrier to elongation when drawing at low temperature, we looked for morphological differences between the low- and high-draw ratio sam-

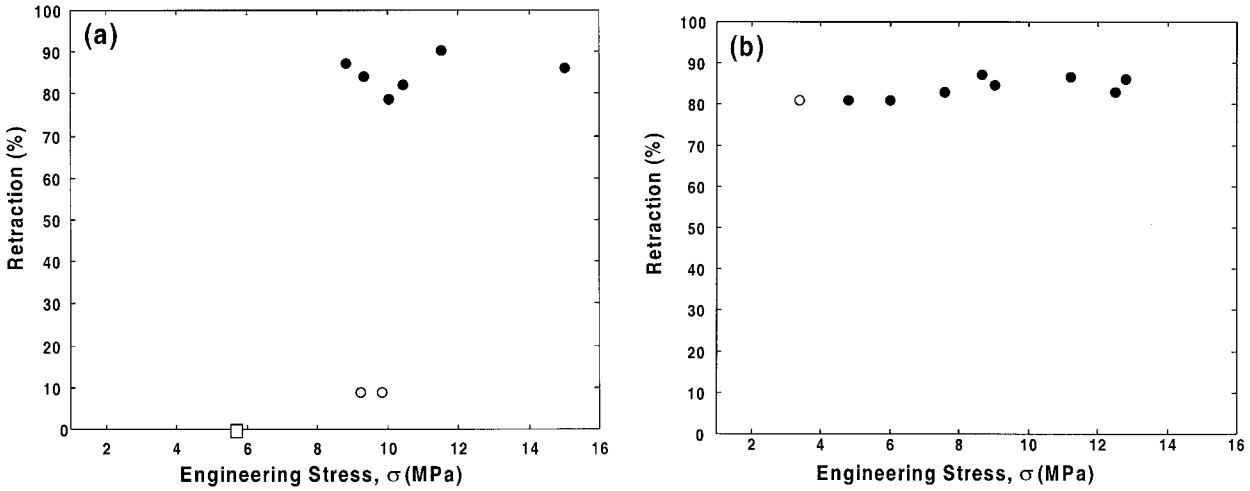

Figure 5 Percent retraction, R, versus engineering stress for D60 drawn at (a) 60°C and (b) 90°C. Open square represents $\lambda = 1.0$; circles represent draw ratios greater than 1.0.

ples. For this, we use SALS to characterize the spherulitic structure within the materials. Undeformed spherulites were deemed to exist in the samples when the SALS pattern was a clear four-lobed pattern (four-leaf-clover type) typical for spherulites.[17] As the draw ratio increases within any sample set, the SALS pattern gradually changes from the four-lobed pattern to a pattern of extended lobes. The lobes shrink in the direction parallel to the applied stress and extend in the direction perpendicular to the applied stress. Finally, the SALS pattern evolves to two nearly straight parallel lines. When the straight-line pattern was dominant, the sample was classified as having no spherulites. Results of SALS were shown in Figure 4, where open symbols represent samples in which spherulites were observed, and solid symbols represent samples in which spherulites no longer could be observed. Generally, spherulites existed in samples that had been drawn only to very low draw ratios from 1.1 to 1.4. The exception is only the C80 sample [Fig. 4(b)], which still contained spherulites at a draw ratio of 2.0. In both D60 and C80, once the draw ratio exceeded 2.5, SALS showed that spherulitic structures were not observed.

Molecular retraction experiments were performed to determine the reversibility of the extension of a drawn sample's amorphous chains. When a drawn sample is heated above its melting point, the crystals are melted and no longer serve as physical crosslinks (i.e., once the crystals are gone, the amorphous phase tends to relax its extended chain conformation). If the drawing process produced purely elastic deformation of the amorphous material, the amorphous chains will now relax to a predrawn length. On the other hand, if the drawing process produced chain slippage and disentanglement, leading to purely plastic deformation of amorphous material, the amorphous chains will be unable to retract to a predrawn length. By using the parameter, R, to characterize the state of the deformation, in the limit of complete retraction ($R = 100\%$), deformation is completely elastic, and elongation occurred by a reversible stretching of the molecular network. In the limit of no retraction ($R = 0\%$), deformation is completely plastic, and elongation occurred by an irreversible slippage of the chains past one another or by chain breakage.

Figure 5(a,b) show plots of percentage retraction versus applied stress for D60 drawn at 60 and 90°C, respectively. Circles represent drawn samples, and the open square represents a sample that did not draw at the stress and temperature applied. The undrawn sample is representative of the original as-pressed material and illustrates that the compression molding operation itself introduced no significant elastic deformation to the specimens. At 60°C, the drawn samples having low retraction, $R < 10\%$ (marked with open circles), were those with low draw ratios, in which spherulites were observed by light scattering [see Fig. 4(a)]. Higher retraction, from 80 to 90%, is observed in samples that had larger draw ratios, no spherulites, and most of which were

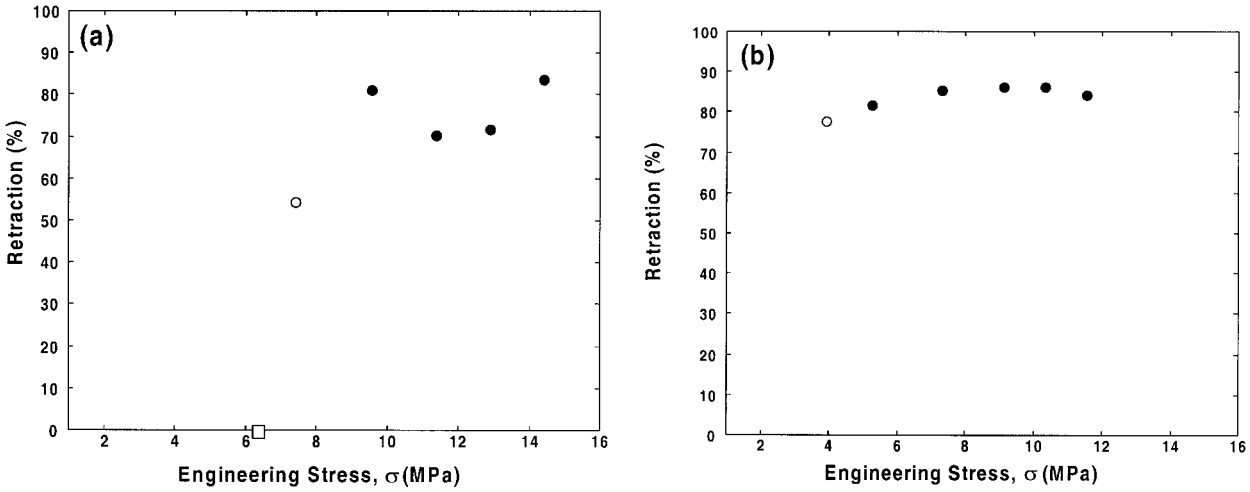

Figure 6 Percent retraction, R, versus engineering stress for C80 drawn at (a) 60°C and (b) 90°C. Open square represents $\lambda = 1.0$; circles represent draw ratios greater than 1.0.

drawn at higher stresses beyond the drawing barrier.

In Figure 5(b), at a higher drawing temperature of 90°C, only high retraction was observed, with R ranging from 80 to 90% for all samples. Here, even the sample that showed spherulitic structure (the data point at stress of 3.2 MPa, marked with an open circle) retracted by 80%.

Figure 6(a,b) shows plots of percentage retraction versus applied stress for C80 drawn at 60 and 90°C, respectively. Again, circles represent drawn samples, and the open square represents a specimen that did not draw at the stress and temperature applied. At T_d = 60°C, retraction of C80 was more scattered that that of D60 at the same temperature ranging from 55 to 80%. All C80 samples had higher retraction percentages when drawn at 90°C than when drawn at 60°C. In comparison to D60, C80 retracted to a lesser extent than D60 when comparing samples drawn at the same temperature and with the same range of drawing stress. On the basis of draw ratio, C80 drew to higher draw ratios than D60, but retracted less. These results taken together suggest that chain slippage occurs to a greater extent in C80 than in D60. Chain slippage causes C80 to draw to larger draw ratios at the same conditions of temperature and stress, but the deformation of the amorphous chains is more plastic than elastic, leading to poorer recovery in the retraction experiments.

Small-Angle X-ray Scattering Analysis

SAXS results support the existence of highly oriented lamellae in drawn samples. Figure 7(a–c) shows two-dimensional SAXS patterns for D60 drawn at 90°C. In the figure, the samples were oriented with the drawing direction horizontal. The undrawn sample's SAXS pattern (which is not shown in the figure) consists of a uniform ring. As draw ratio increases, the SAXS pattern changes from a uniform circular pattern to the ellipse-shaped pattern shown in Figure 8(a) (λ = 1.4), with the short axis parallel to the draw direction. In Figure 8(a), the SAXS intensity is concentrated on the meridian and diminished on the equator. This specimen showed strong spherulitic structure in SALS. As the draw ratio increases to λ = 3.3 [Fig. 8(b)], the SAXS pattern becomes a butterfly, characteristic of highly oriented lamellar stacks. Now there is no intensity on the equator, and two strong meridional spots are seen along with the beginning of layer line structure. When the draw ratio increases to λ = 6.5, Figure 8(c) shows a pattern dominated by void scattering, which is located around the center beam stop. Along with the void scattering, very weak intensity in a four-point layer line pattern was observed on the original prints but cannot be seen on the reproductions.

The SAXS intensity in Figure 8(a) represents a microstructure comprising spherulites having aligned lamellae. When the SAXS pattern changes from a ring to an ellipse, the WAXS results show intensity changing from a ring (unoriented crystals) to equatorial spots. As the molecular chain axis begins to align along the stress direction, the crystallographic a-axis becomes perpendicular to the stress direction.[2,5,6] Once

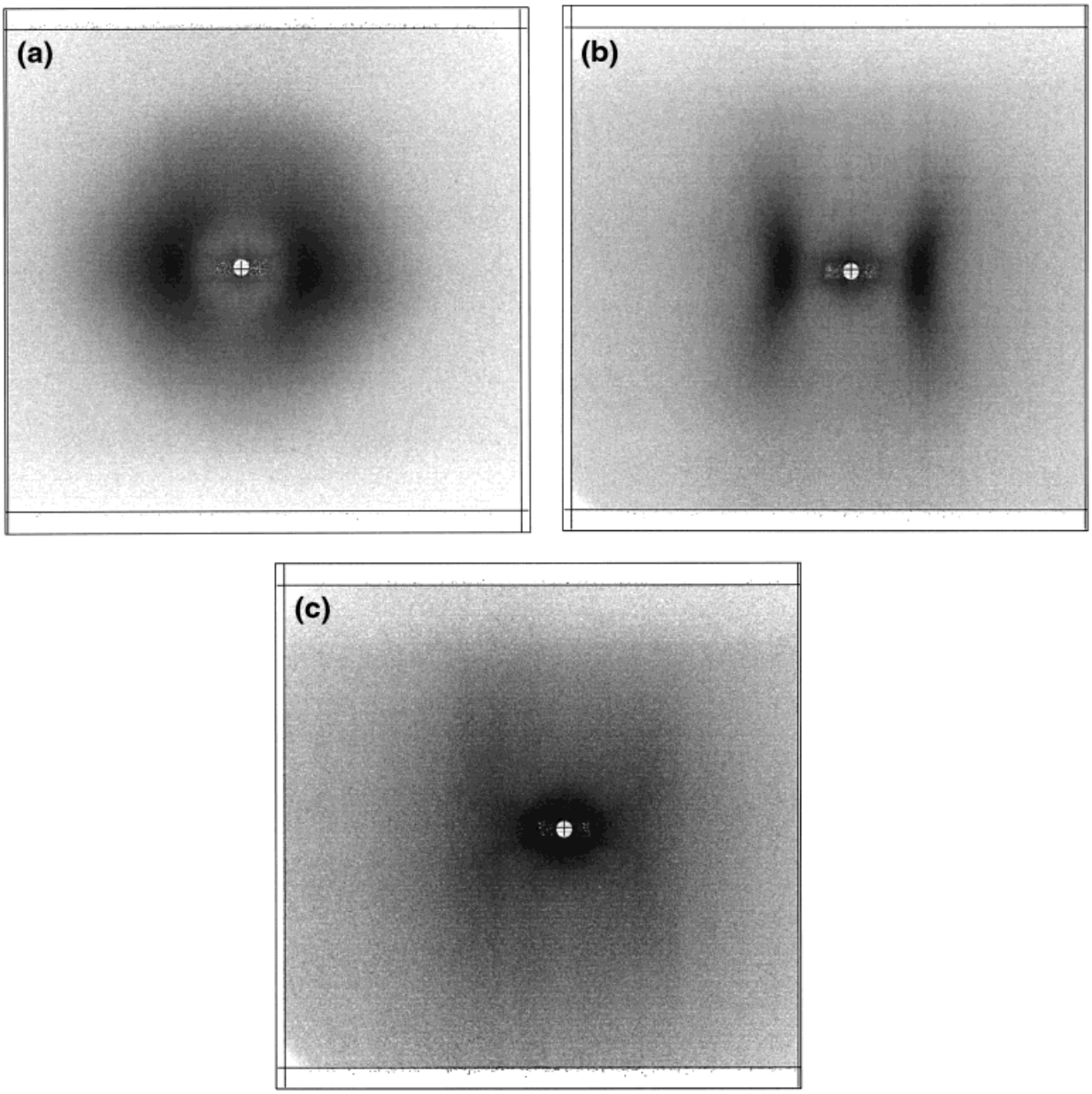

Figure 7 SAXS patterns for D60 drawn at T_d = 90°C at draw ratios: (a) 1.4; (b) 2.6; (c) 4.5.

SALS reveals that the spherulitic structures are destroyed, SAXS shows a two- or four-spot layer line pattern. Similar results were obtained for C80. We note that unlike the results of Butler et al. on *z*-PE,[12] which showed very strong void scattering at low strains of 0.18 (λ = 1.18), we observed void scattering only at the very highest draw ratios, λ = 5.6 or greater for D60 and λ = 7.2 for C80.

The major difference between the two materials from the standpoint of microstructure is that the lamellar alignment occurs at higher draw ratios in C80 than in D60. In other words, it takes a higher draw ratio in C80 to see the same degree of lamellar alignment that occurs in D60 at lower draw ratio. This concurs with the previous data of Figure 4, which showed that it is easier to draw C80 and higher draw ratios were achieved in the C80 than in the D60 with the same applied stress. The explanation for both effects is the reduced molecular weight and lower number density of entanglements in the C80. It is easier to elongate

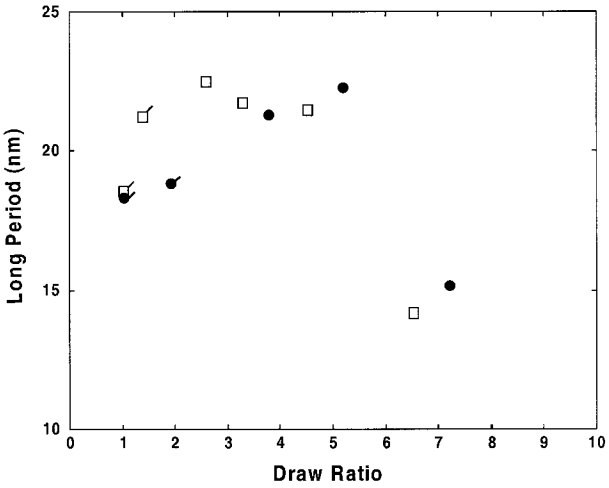

Figure 8 Long period versus draw ratio for D60 (squares) and C80 (circles) drawn at 90°C. The symbols at $\lambda = 1.0$ represent undrawn materials. Samples containing spherulites are indicated by symbols with flags.

C80 than D60, but more difficult to orient the crystallites, because more chain slippage is occurring in C80.

From the SAXS data, the long period, or interlamellar stack periodicity, is obtained. To characterize the position of the long period, we use the intensity maximum position, either on the equator of the two-spot pattern or at the center of the lobes in a four-point layer line pattern. In Figure 8, we plot the long period as a function of draw ratio for D60 (squares) and C80 (circles) drawn at 90°C. The long period of undrawn sample is shown for comparison as the point at $\lambda = 1.0$ using similar symbols. The symbols marked additionally with flags represent samples in which spherulites are observed by SALS. Both undrawn samples have about the same long period. Once drawing begins, the long period first increases, sharply for D60 and more gradually for C80. These results are consistent with the reduced ability of C80 crystals to orient due to chain slippage. The increase in the long period with draw ratio indicates an increase in the average spacing between adjacent lamellae. Beyond a draw ratio of about 5.6 (for D60) and 6.0 (for C80), the long period drops dramatically in both materials. It is in these samples that void scattering is seen, and the intensity in the layer lines of the SAXS pattern becomes extremely weak. These results suggest that the lamellar crystals are being converted into fibrillar crystals, and the remaining lamellar stacks are few in number (giving very weak SAXS intensity) and comprise poor crystals with shorter average stack periodicities.

DISCUSSION

We now consider the role of spherulites and the crystalline lamellae on the ability of samples to draw and to retract after drawing. Prior to drawing, both C80 and D60 samples have spherulitic microstructure. Depending on drawing conditions, this microstructure may or may not remain in the drawn samples. In general, at the lower drawing temperatures (50 and 60°C), the samples that were drawn to a lesser extent (i.e., drawn at low drawing stresses, resulting in lower draw ratio and insignificant amount of necking) were observed to contain spherulites after drawing. These samples also had the smallest molecular retraction. At low T_d, the spherulites remain largely intact when low stresses are applied, similar to the results of Hoff and Peltzbauer,[9,10] who found that zone drawing of *z*-PE left spherulites undeformed prior to neck formation. After necking, the spherulites became extended and the lamellae oriented with their *c*-axes parallel to the direction of applied stress.[9,10] We suggest that at low drawing stresses, the resultant low draw ratio is attributed to drawing of interspherulitic amorphous chains, which is consistent with studies on *z*-PE,[5] in which spherulites were observed to deform first at their boundaries. The spherulite boundaries contain polymer material that is less able to crystallize and is rejected ahead of the growth front. The low retraction implies that the interspherulitic, low-modulus amorphous phase is deforming plastically when extended under these conditions of low drawing stress and low drawing temperature.

When the drawing stress is increased at low drawing temperature, spherulitic superstructure disappears. SALS shows that the spherulites are first deformed, and then ultimately destroyed, by the drawing process as stacked lamellar crystals are converted into fibrillar crystals. According to the work of Butler and Donald on *z*-PE, "fibrillation may only proceed after lamellar disruption."[23] This disruption of lamellae occurs first by interlamellar separation in the equatorial regions and by micronecking in the meridional regions.[6] Stress in the equatorial region stretches the intraspherulitic amorphous material that resides between, and is highly entangled with, the crystal lamellae. As this material becomes stressed, the

adjacent lamellae will become separated. Both interlamellar separation and micronecking are likely to result in the decrease in degree of crystallinity observed in the samples drawn at low temperature, compared to the undrawn samples. The larger draw ratios and larger molecular retractions measured at high drawing stresses suggest more elastic deformation of intraspherulitic amorphous chains.

At low T_d, it is only beyond a critical stress that spherulitic structure disappears. A natural thought is that the spherulites play the role of a barrier to elongation at low temperatures until a critical stress is reached. Initially, at low T_d, the lower modulus, interspherulitic amorphous phase extends and the sample elongates to low draw ratio, spherulites intact. During drawing, stress is transferred to the higher modulus crystalline phase. When the critical drawing stress is reached, elongation can proceed via deformation of the intraspherulitic amorphous phase. This disruption of the spherulitic superstructure can occur at low T_d only by application of large drawing stresses.

At high T_d (70–100°C), spherulite disruption is facilitated and occurs at much lower applied stress levels. The zone-drawing treatment must certainly melt a portion of the least perfect crystallites forming the spherulites. The DSC scans of Figure 1 show that the melting endotherm is very broad and has a low-temperature tail extending down even to the lowest temperatures used in zone drawing. The amount of crystallites melted will increase with an increase in T_d. Reduction in the number of the thermoreversible crystalline crosslinks by melting at T_d is one likely cause of the increased ability to draw at higher temperatures. The degree of crystallinity increases slightly after drawing, but these materials still have low overall levels of crystallinity, close to 0.34 after drawing at elevated temperatures. Therefore, there is a very large fraction of amorphous inter- and intraspherulitic material. The intraspherulitic (interlamellar) amorphous chains do not irreversibly slip or disentangle when extended. Rather, they deform elastically resulting in the large molecular retraction measured in the samples drawn at high temperature.

CONCLUSION

The zone-drawing behavior of metallocene polyethylene depends on the molecular chain length, as it does in conventional Ziegler–Natta-catalyzed PEs. C80, which has shorter chains and higher melt flow index, was easier to draw than D60, giving larger draw ratios for the same drawing stress and temperature. A larger amount of chain slippage occurred in C80, resulting in a smaller degree of molecular retraction and in weaker crystalline orientation under the same drawing conditions. Both D60 and C80 materials had about the same overall initial crystallinity. Crystalline fraction decreased upon drawing at low temperature and increased slightly when T_d exceeded 80°C. Spherulites were observed only in samples drawn to low extension ratios. As drawing progresses, spherulites are disrupted and lamellar separation and slip become the dominant mechanism for deformation. In the properties studied here, *m*-PE behaved predictably and similarly in its general trends to *z*-PE.

This research was supported in part by the National Aeronautics and Space Administration under Grant NAG8-1460 and by the U.S. Army Research Office under Grant DAAH04-96-1-0009. Tufts University undergraduate students D.M.V. and E.O. thank the Physics and Astronomy Department Undergraduate Research in Physics Program for partial support. The authors thank Dr. Robert Bamberger of Exxon for supplying the metallocene PE used in this study.

REFERENCES

1. Keller, A. in Growth and Perfection of Crystals; Doremus, R., Roberts, B., Turnbull, D., Eds.; Wiley: New York, 1958; p 499.
2. Keller, A. J Polym Sci 1955, 15, 31.
3. Pope, D.; Keller, A. J Polym Sci, Polym Phys Ed 1975, 13, 533.
4. Pope, D.; Keller, A. J Polym Sci, Polym Phys Ed 1976, 14, 821.
5. Hay, I.; Keller, A. Kolloid Z Z Polym 1965, 204, 43.
6. Lin, L.; Argon, A. J Mater Sci 1994, 29, 294.
7. Kunugi, T.; Oomori, S.; Mikami, S. Polymer 1988, 29, 814.
8. Yeh, J.-T.; Chang, S.-S.; Yen, M.-S. J Appl Polym Sci 1998, 70, 149.
9. Hoff, M.; Pelzbauer, Z. Polymer 1992, 33, 4158.
10. Hoff, M.; Pelzbauer, Z. Polymer 1991, 32, 999.
11. Russell, K.; Hunter, B.; Heyding, R. Polymer 1997, 38, 1409.
12. Butler, M. F.; Donald, A. M.; Ryan, A. J. Polymer 1998, 39, 39.
13. Robert Bamberger, private communication, 1997.
14. Aihara, Y.; Cebe, P. Polym Eng Sci 1994, 34, 1275.

15. Garrett, P.; Grubb, D. T. Polym Commun 1988, 29, 60.
16. Wunderlich, B. Macromolecular Physics; Academic Press: New York, 1980; Vol. 3, p 58.
17. Haudin, J. M. Optical Studies of Polymer Morphology; Meeten, G. H., Ed., Optical Properties of Polymers; Elsevier Appl. Sci.: London, 1986.
18. Capel, M.; Smith, G.; Yu, B.; Rev Sci Instrum 1995, 66, 2295.
19. Grubb, D. T. J Mater Sci Lett 1984, 3, 499.
20. Wunderlich, B. Macromolecular Physics; Academic Press: New York, 1973; Vol 1, p 97.
21. Sabbagh, A.; Lesser, A. J. J Polym Sci, Polym Phys Ed 1999, 37, 2651.
22. Exxon Product Data Sheet, for EXCEED PE 350D60, 1999.
23. Butler, M. F.; Donald, A. M. J Mater Sci 1997, 32, 3675.